

Study and formation of vesicle systems with low polydispersity index by ultrasound method

J. Pereira-Lachataignerais^{a,*}, R. Pons^a, P. Panizza^b, L. Courbin^b,
J. Rouch^b, O. López^a

^a *Departamento de Tecnología de Tensioactivos, Instituto de Investigaciones Químicas y Ambientales de Barcelona (I.I.Q.A.B.)-Consejo Superior de Investigaciones Científicas (C.S.I.C.), Calle Jorge Girona 18-26, 08034 Barcelona, Spain*

^b *Centre de Physique Moléculaire Optique et Hertzienne (CPMOH), Université de Bordeaux I, Centre National de la Recherche Scientifique (CNRS), 351, Cours de la Liberation, 33400 Talence, France*

Received 25 February 2005; received in revised form 25 January 2006; accepted 25 January 2006
Available online 21 February 2006

Abstract

The formation of liposomes with low polydispersity index by application of ultrasounds was investigated considering methodology specifications such as sonication time and sonication power. Phosphatidylcholine (PC) liposomes were formed by the evaporation–hydration method. The vesicles were sonicated using several sonication conditions. The liposomes were then characterized by dynamic light scattering (DLS) and freeze–fracture electron microscopy (FFEM). Correlation functions from DLS were treated by cumulants method and GENDIST to obtain the mean radius and polydispersity index. These calculations allowed to fix an optimal sonication time (3000 s) and a useful interval of ultrasound power between 39 and 91 W. DLS and FFEM results confirmed that vesicle size, lamellarity and the polydispersity index decreased with the increase of sonication power. Thus, we propose a systematic method to form liposomes in which the physical characteristics of the vesicles may be controlled as a function of sonication time and power.

© 2006 Elsevier Ireland Ltd. All rights reserved.

Keywords: Liposome; Ultrasound; Freeze–fracture electron microscopy; Dynamic light scattering

1. Introduction

Liposomes or lipid bilayer vesicles have been the subject of numerous studies because of their importance as models for more complex biological membranes, their potential use as microencapsulators for drug

delivery and their applications in cosmetics (Sackmann, 1995; Gregoriadis, 1995; Teschke and de Souza, 2002). Depending on the preparation methods, these self-assembled macromolecular aggregates can exist as uni- or multilamellar lipid bilayer systems (Baszkin and Norde, 2000). Some of these methods are based on the removal of surfactant from phospholipid–surfactant mixed micelles by dialysis (Classen and Spooner, 1995) or by dilution (New, 1990). However, the complete removal of surfactant from the resulting vesicles is difficult and dependent on the type of surfactant (Ollivon et al., 2000). This problem is eliminated by use of methods that do not involve the lipid–surfactant mixture. Thus,

Abbreviations: DLS, dynamic light scattering; FFEM, freeze–fracture electron microscopy; PC, phosphatidylcholine; PI, polydispersity index

* Corresponding author. Tel.: +34 93 400 61 00x301;
fax: +34 93 204 59 04.

E-mail address: jlpten@iiqab.csic.es (J. Pereira-Lachataignerais).

the hydration of a lipid film and the reverse evaporation phase methodologies have resulted useful (Cladera et al., 1997). The method based on freeze–thaw cycles is also used for vesicle formation (Monnard et al., 1999; Kaasgaard et al., 2003). However, this method can cause the fragmentation as well as the fusion of the vesicles depending on the lipid mixtures (Traikia et al., 2000). In general, all these methodologies do not give a population with homogeneous size and lamellarity. Thus, homogeneous populations of unilamellar vesicles can be prepared by extrusion, centrifugation or sonication of multilamellar vesicles (Classen and Spooner, 1995; Ollivon et al., 2000). These methods can involve some difficulties, such as the sample loss during manipulation, the prolonged time to obtain the final sample and the possible aggregation and/or phase separation. With the aim of minimizing these problems we propose a systematic study of the preparation of the lipid vesicles using sonication. Although the use of ultrasound in the formation of liposomes is not new (Kiyoshi et al., 1992), a detailed description of the methodology specifications, such as the optimal sonication power and sonication time, is still lacking. Thus, this study describes the sonication conditions to obtain systems of lipid vesicles with low polydispersity and lamellarity.

Electron microscopy and light scattering have been often used to determine vesicle size. In fact, in earlier papers our group studied the structural changes in liposome systems caused by surfactants using freeze-fracture electron microscopy (FFEM) and dynamic light scattering (DLS) (López et al., 1998a,b; Cócera et al., 2003). These techniques have reported useful and complementary information as regard to the characterization of the systems containing different lipid structures. Thus, whereas DLS offer a good statistics in situ measurements, and simple preparation procedure the FFEM give a more detailed view of the structures.

In this work, we investigated the size changes of liposomes as well as the polydispersity and lamellarity of the systems as a function of the ultrasound power applied. Information about the vesicle size distribution and the polydispersity was obtained through the cumulants (Johnson and Gabriel, 1994) and REPES methods calculation (Schillén et al., 1994) from correlation functions obtained by DLS. FFEM technique was used to characterize lamellarity and vesicles size. A precise knowledge of the effect of ultrasounds on these parameters would be useful to predict and control the characteristics of lipid vesicles currently used in biotechnical applications and biophysical investigations.

2. Materials and methods

Lipoid S-100, whose main component (>96%) is soybean phosphatidylcholine (PC), the remaining corresponds to 1.7% nonpolar lipids, 0.5% triglycerides, 0.5% lysophospholipids and 0.7% corresponds to water. The phospholipid was obtained from Lipoid GmbH (Ludwigshafen, Germany). Chlorophorm were purchased from Merck. Polycarbonate membranes and membrane holders were purchased from Nucleopore (Pleasanton, CA, USA).

2.1. Liposome preparation

A lipid film was formed by removing the chlorophorm by rotary evaporation from a containing Lipoid S-100 solution. Liposomes using different PC concentrations, 3.75, 5.62 and 7.50 g/L, were obtained by hydration of the lipid film with salt solution 0.5 g/L NaCl. In some cases these solutions were extruded five times through 800 nm polycarbonate membranes.

2.2. Sonication of the liposome solutions

The application of ultrasound was carried out using a high intensity sonicator series Autotune, model 130 W with frequency of 20 kHz and titanium probe diameter 3 mm. The solutions (10 mL) were sonicated by means of different powers, between 26 and 130 W at room temperature. In order to avoid excess heating of the sample, the beaker was immersed in a water bath at 25 °C. The temperature was never above 40 °C in the sample. The sonication was carried out with treatment of 50 min by sections of 10 min: 6 s of pulse and intervals of 1 s. The capacity of beakers for sonication was 15 mL with dimensions 6.5 cm height and 1.5 cm diameter.

2.3. DLS experiments

The size of vesicles was determined by using the photon correlator spectrometer equipped with an Argon laser with $\lambda = 488$ nm and refrigerated by air. The correlator used was ALV5000 and the measurements were performed at several scattering angles between 60° and 140° with sample time of 0.2 μ s and 25 °C.

2.4. Treatment of DLS data for radius calculations

In order to analyze DLS results we considered that the particles were moving in a continuous medium by Brownian motion. Homodyne experiments, which involve the

use of the relation (1), were carried out with the equipment of DLS:

$$\tau = \frac{1}{2Dq^2} \quad (1)$$

in which τ is the relaxation time, D the diffusion coefficient and q is the scattering vector defined by Eq. (2).

$$q = \frac{4\pi n}{\lambda} \sin\left(\frac{\theta}{2}\right) \quad (2)$$

where n is the refraction index, λ the wavelength of light and θ is the scattering angle.

Correlation functions $g^{(2)}(\tau)$, obtained by DLS, are expressed by the following equation:

$$g^{(2)}(\tau) = 1 + A \exp(-2Dq^2\tau) \quad (3)$$

The fit of the experimental correlation functions by Eq. (3) led to the determination of τ values at six different scattering angles, between 60° and 140° . Fig. 1 shows the correlation function obtained at scattering angle 70° corresponding to a sample concentration of 3.75 g/L PC, sonicated with 91 W of power.

In order to determine the diffusion coefficient, D , τ values were plotted versus $1/q^2$ for every sonication power. The slope of curve in the linear fit corresponds to $1/(2D)$ considering Eq. (1) and the scattering vector, q , was calculated by Eq. (2).

Given the values D and taking into account the Stokes–Einstein Eq. (4), the particle radius in solution can be calculated, the particle radius in solution should be replaced by the hydrodynamic radius of the particle:

$$D = \frac{kT}{6\pi\eta R} \quad (4)$$

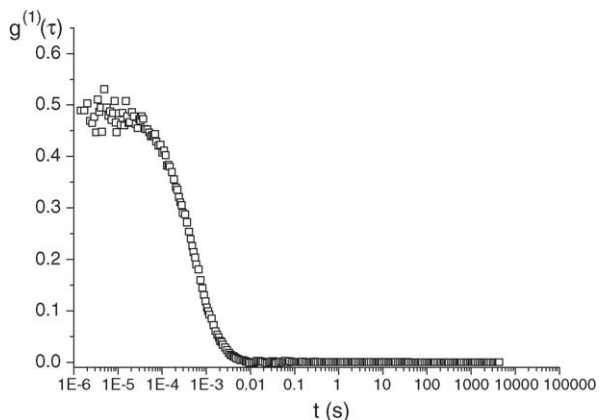


Fig. 1. The correlation function obtained at scattering angle 70° corresponding to a sample concentration of 3.75 g/L PC, sonicated with 91 W of power.

where $k = 1.3807 \times 10^{-23}$ J/K is the Boltzmann constant, $T = 298$ K and $\eta = 10^{-3}$ Pa s is the viscosity of water.

2.5. Treatment of DLS data for polydispersity index calculation

Polydispersity index was calculated using the cumulants method (Johnson and Gabriel, 1994) fitting the functions $Y(\tau)$ to polynomials of second order.

$$Y(\tau) = \ln[g^{(2)}(\tau) - 1]^{1/2} = \frac{1}{2} \ln\beta + \sum_{m=1}^{\infty} K_m \frac{(-\tau)^m}{m!} \quad (5)$$

Eq. (5) defines $Y(\tau)$, which is related with the correlation function obtained by DLS (Eq. (3)). Where β is a factor of order unity and K_m cumulants which have the following values:

$$K_1 = \langle \Gamma \rangle, K_2 = \mu_2, K_3 = \mu_3, \dots, K_m = \mu_m$$

$\langle \Gamma \rangle$ is the average relaxation rate and μ_2 is the variance of distribution. From Eq. (6) the polydispersity index, P , was calculated.

$$P = \frac{\mu_2}{\langle \Gamma \rangle^2} \quad (6)$$

2.6. Data analysis to obtain distribution functions through GENDIST program

GENDIST is an interactive program for the analysis of homodyne DLS data. A copy of this program can be obtained from Dr. Robert Johnsen at Uppsala University, Sweden, see <http://www.fki.uu.se/gendist.htm>. The program can fit three different models: a form free model and a fixed form model for the distribution for relaxations and a fixed form for the intensity autocorrelation function. We have used the form free model. All the models include an adjustable baseline and an adjustable β .

The DLS data were analyzed by nonlinear regression procedures. The model used in the fitting procedures are expressed with respect to $g^{(1)}(\tau)$, while the fitting was performed with respect to the measured $g^{(2)}(\tau)$, described as

$$g^{(2)}(\tau) - 1 = \beta |g^{(1)}(\tau)|^2 \quad (7)$$

where β is a nonideality factor, which accounts for the deviation from ideal correlation. $g^{(1)}(\tau)$ can be written as the Laplace transform of distribution of relaxation rates, $G(\Gamma)$:

$$g^{(1)}(\tau) = \int_0^{\infty} G(\Gamma) \exp(-\Gamma\tau) d\Gamma \quad (8)$$

Table 1

Values corresponding with the polydispersity index (PI) calculated by cumulants method and σ_r (standard relative deviation) and R_G (radius), calculated by GENDIST, for every sonication power and PC concentrations: 3.75, 5.62 and 7.5 g/L

Power (W)	3.75 g/L			5.62 g/L			7.5 g/L		
	R_G (nm)	PI	σ_r	R_G (nm)	PI	σ_r	R_G (nm)	PI	σ_r
39	105.0	0.36	0.87	103.8	0.22	0.87	96.1	0.12	0.87
52	82.0	0.10	0.83	90.1	0.18	0.94	–	–	–
65	74.0	0.17	0.77	80.0	0.11	0.82	64.5	0.14	1.13
78	62.5	0.11	0.66	63.7	0.32	0.61	69.0	0.13	0.67
91	58.8	0.10	0.51	62.5	0.10	0.67	63.3	0.10	0.37

where Γ is the relaxation rate and t is the lag time. For relaxation times, τ , Eq. (8) will be expressed as

$$g^{(1)}(\tau) = \int_0^\infty \Gamma A(\Gamma) \exp\left(-\frac{\tau}{\Gamma}\right) d(\ln \Gamma) \quad (9)$$

where $\tau A(\tau) \equiv \Gamma G(\Gamma)$ in the logarithmic scale. $\tau A(\tau)$ was obtained by regularized inverse Laplace transformation (RILT) of the dynamic light scattering data using a constrained regularization calculation algorithm called REPES as incorporated in the analysis package GENDIST. This algorithm directly minimizes the sum of the squared differences between experimental, $g^{(2)}(\tau)$, and calculated, $g^{(1)}(\tau)$, functions (Schillén et al., 1994). The hydrodynamic particle radius (R_G in Table 1) was obtained from the distribution of relaxation time through Eqs. (1) and (4).

2.7. Transmission electron microscopy experiments

Freeze-fracture electron microscopy (FFEM) pictures were taken from liposome dispersions. About 1 μL of solution of liposomes was sandwiched between two copper platelets using a 400-mesh gold grid as the spacer. Then, the samples were cryofixed by dipping into nitrogen-cooled liquid propane at -180°C and fractured at -110°C and 5×10^{-7} mbar in a BAF-060 freeze-etching apparatus (BAL-TEC, Liechtenstein). The replicas were obtained by unidirectional shadowing with 2 nm of Pt/C and 20 nm of C, they were floated on distilled water, collected on 300-mesh copper grids coated with collodion film and examined in a Hitachi H-600 transmission electron microscopy at 75 kV (López et al., 1998a).

3. Results

3.1. Optimization of the sonication conditions

Liposome dispersions were treated using different sonication powers. DLS measurements were performed

at several scattering angles on these dispersions. Fig. 2 shows the functions where $\tau A(\tau)$ is plotted versus $\log(\tau)$, at a scattering angle of 75° . These curves correspond to different dispersion liposomes, 3.75 g/L PC, formed using sonication powers of 39, 52, 65, 78 and 91 W for 3000 s. In the graphic is clearly observed a modal distribution of particles according with a single relaxation mode. This fact, that was observed regardless the scattering angle, is associated with the presence of only one population of particles. When the liposome dispersions were sonicated with the maximum power of the equipment (130 W) the correlation functions showed two relaxation times. Fig. 3 shows the distribution functions that justified this behavior. The experiment at the maximum sonication power, 130 W, was reproducible. However, the interpretation of this observation is difficult given that this double relaxation was not observed either at all scattering angles and/or at lower sonication powers. Considering these results and, in order to avoid wrong interpretations, an interval of ultrasound power, in which only one relaxation time was detected, was chosen to perform the liposome sonication. Thus, the working interval of ultrasound power was fixed between 39 and 91 W.

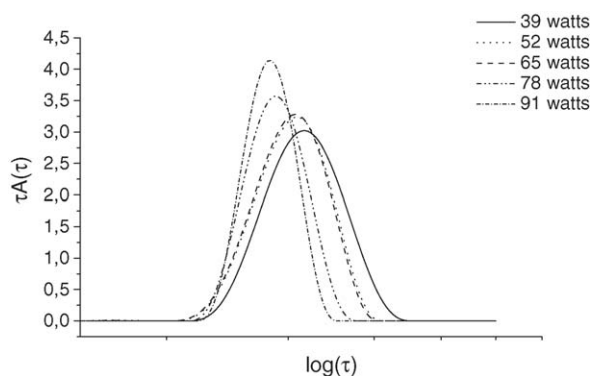


Fig. 2. Correlation functions obtained by DLS with scattering angle 70° of samples sonicated at different powers between 39 and 91 W. Liposome concentrations 3.75 g/L of PC.

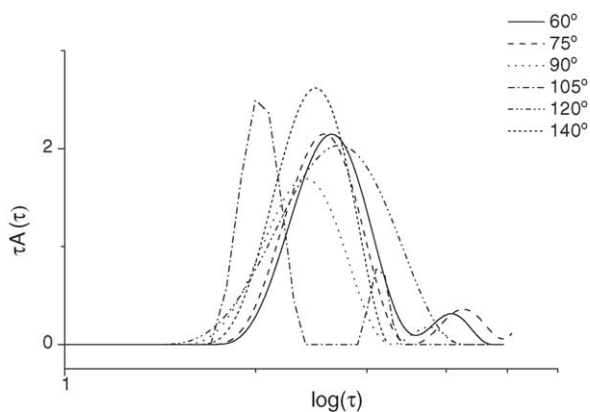


Fig. 3. Correlation functions of liposome dispersion 3.75 g/L of PC sonicated at 130 W at different scattering angles.

Optimum sonication time was also determined. The variation of the vesicles size with sonication time at different fixed sonication powers was analyzed. Fig. 4 shows the vesicle size, obtained by GENDIST, after increasing sonication times using constant sonication powers: 52, 78 and 91 W, for the system containing a PC concentration of 3.75 g/L. This figure shows a decrease of the particle radius with the increase of the sonication time until a plateau radius was obtained after about 2200 s of sonication. These results also show that the vesicle radius at the plateau decreased when the sonication power increased. Some experiments were performed using higher PC concentration and the size stabilization time was always between 2000 and 2500 s, at least in the PC concentration studied in this work. In any case, in order to ensure that the sonication time was enough to form the vesicles with stable size, a slightly higher sonication time, 3000 s, was considered appropriate to

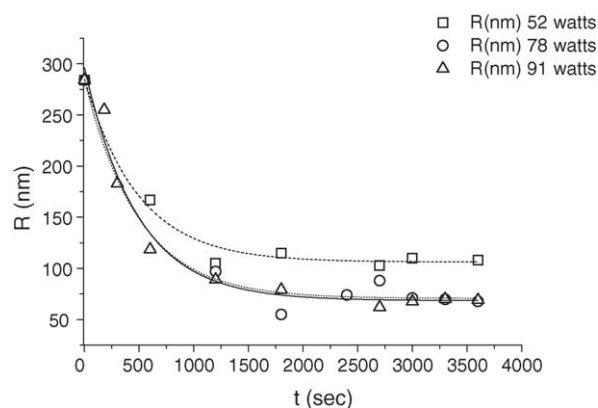


Fig. 4. Variation of the vesicles size with sonication time at different fixed sonication powers: 52, 78 and 91 W. Lines correspond to fitted data according to Eq. (14).

perform the ultrasound treatment of the liposome dispersions.

3.2. Dependence of liposome size and PI as a function of the sonication power and concentration

Using a sonication time of 3000 s and increasing sonication powers from 39 to 91 W, a decrease of the vesicles size was observed. Fig. 5 shows these size variations for three liposome solutions at PC concentrations of 3.75, 5.72 and 7.50 g/L. Considering a constant sonication power, higher values of vesicle size could be expected for liposome dispersion with higher PC concentration, given that the same ultrasound energy has to be distributed in a bigger amount of material. However, this effect was not observed neither in experimental or calculated values. The size was similar for three solutions sonicated at the same power. Thus, in this concentration range the final size of particles seems to be independent of the liposome concentration. Additional size measurements carried out after 72 h verified the stability of the liposomes and the reproducibility of the results.

Table 1 shows the PI, the radii (R_G) of the vesicles and their relative deviation, all of these parameters decrease with the increase of sonication power. The PI of the samples, calculated by cumulants method, is associated to a different vesicle size distribution. The relative deviations were obtained by GENDIST program and are equivalent to polydispersity.

Fig. 6 shows size distribution curves calculated using GENDIST program (Schillén et al., 1994) from the autocorrelation functions obtained by DLS at scattering angle of 90° using 39 and 91 W of sonication power for the sys-

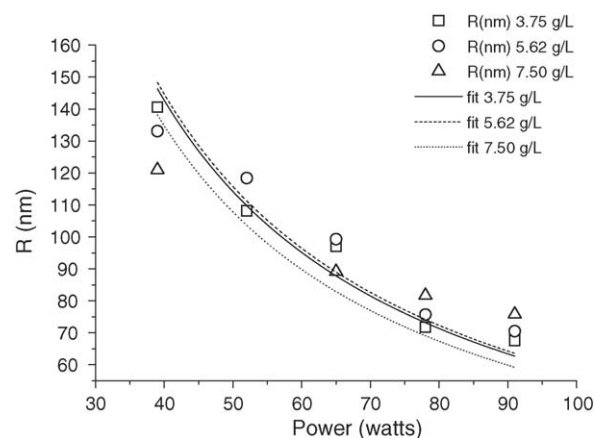


Fig. 5. Radius variations in function of sonication power for the three liposome dispersions PC concentrations: 3.75, 5.62 and 7.5 g/L. Lines correspond to fitted data according to Eq. (15).

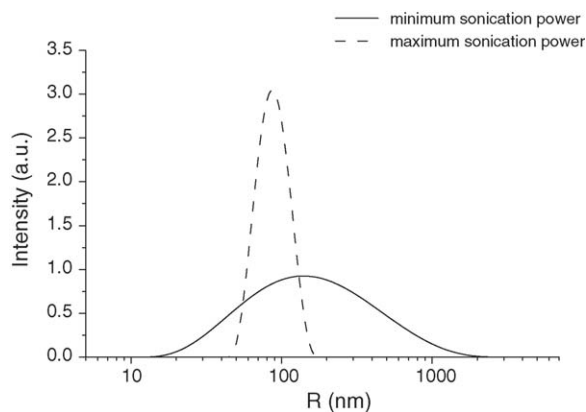


Fig. 6. Size distribution curves corresponding to the samples sonicated at 39 W (minimum sonication power) and 91 W (maximum sonication power).

tem 3.75 g/L. These distribution curves allow to define a range of radii for these values of PI, that is, 30–800 and 60–130 nm for the maximum, 0.36, and minimum, 0.10, values of PI, respectively. In order to fix these

ranges we have only taken into account the particles that contribute to intensity with values above 25 a.u. (Fig. 6).

In Fig. 7, the micrographs show freeze-fractured replicas of a few vesicles corresponding to the sample with PC concentration 3.75 g/L and sonicated at 39 W, these were observed by TEM. These micrographs show variability in size that qualitatively agree with the results obtained from PI measurements. Thus, vesicles with radii about 100 nm coexists with smaller vesicles of about 60 nm (Fig. 7A and B). In general almost all the vesicles visualized are multilamellar.

The sample sonicated at 91 W was also observed by TEM and some of the micrographs are shown in Fig. 8. Only occasionally unilamellar vesicle (Fig. 8A) and multilamellar vesicles with few bilayers (see arrow, Fig. 8B) were observed. The vesicles present in this sample are smaller than those observed in Fig. 7, agreeing with the DLS results. Thus, sizes between 50 and 70 nm of radius are observed. The general observation was in agreement with the PI obtained by DLS.

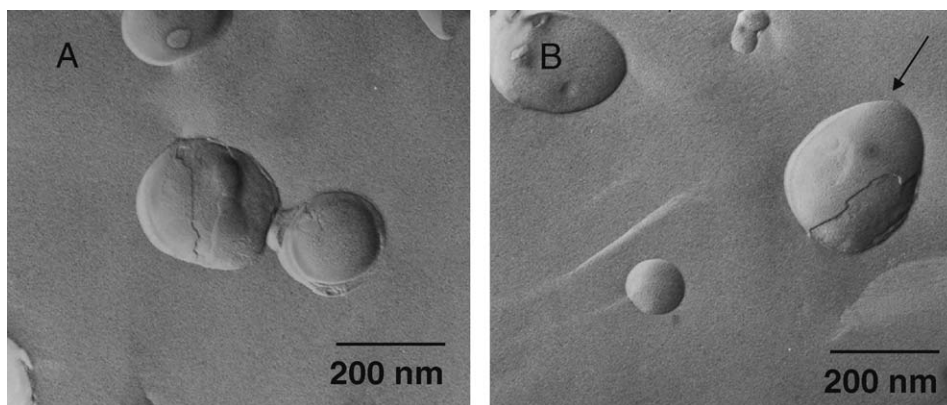


Fig. 7. Micrograph (A) shows two vesicles with certain multilamellarity and micrograph (B) shows a unilamellar vesicle and another one multilamellar (arrow). Both images correspond with the sample 3.75 g/L of PC and sonicated at 39 W.

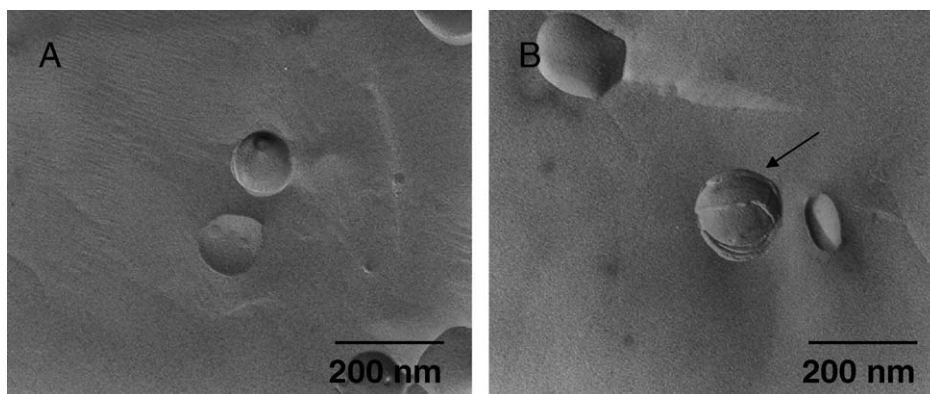


Fig. 8. Micrographs (A and B) corresponding with vesicles sonicated at 91 W. Image (A) shows a unilamellar vesicles and (B) shows a vesicle with low lamellarity (see arrow).

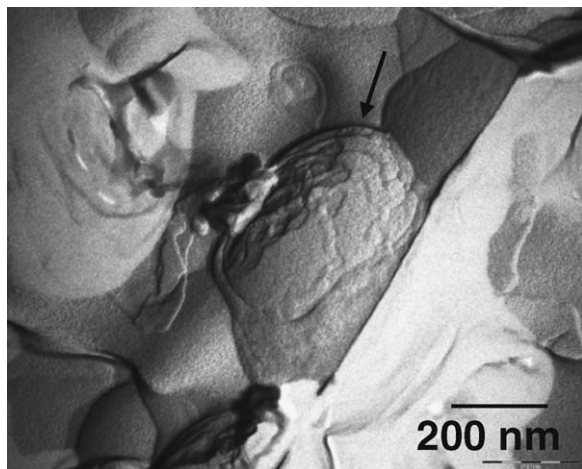


Fig. 9. Picture of vesicles extruded through polycarbonate membranes of 800 nm of diameter showing the multilamellarity of the vesicle (see arrow).

In order to compare the structure of sonicated and unsonicated vesicles some liposomes without ultrasound treatment were visualized. Fig. 9 shows a picture of vesicle extruded through polycarbonate membranes of 800 nm of diameter. This sample was not sonicated. The micrograph shows multilamellar vesicle with radius between 200 and 250 nm (see arrow).

4. Discussion

First of all we seek to analyze the energy necessary to form liposome in order to compare it with the energy inputted by sonication.

The curvature energy per unit area of bilayer (f_c) deduced by Jung et al. (2001) is defined by the following equation:

$$f_c = 2K \left(\frac{1}{R} - \frac{1}{R_0} \right)^2 \quad (10)$$

$$2K = 2\kappa + \bar{\kappa}$$

in which R is the effective radii of curvature, R_0 the spontaneous radii of curvature, $R_0 = \infty$ when the formation of lamellar phase is spontaneous and K is the effective bending constant.

This constant is related with κ , the mean curvature elastic modulus, and $\bar{\kappa}$, the Gaussian curvature elastic modulus. These elastic constants are related with the bilayer organization which should not change in the system studied. Thus, f_c can be calculated using $K \approx 20k_B T$ which is used in literature for phospholipid bilayers (Jung et al., 2001).

The chemical potential is the change in curvature energy per molecule expressed in the following equation:

$$E_{\text{curvature}} = \mu_N = \frac{4\pi R^2 f_c}{N} \quad (11)$$

where $N = 8\pi R^2/A_0$ is the aggregation number and A_0 is the area per molecule (Jung et al., 2001).

Replacing f_c and N in Eq. (11),

$$E_{\text{curvature}} = \mu_N = \frac{K \cdot A_0}{R^2} \quad (12)$$

and applying the parameters of our system, $R = 140$ nm, we obtained the $E_{\text{curvature}} = 2.07 \times 10^{-18}$ J/vesicle. Taking into account that the liposomes concentration is 3.75 g/L and the number of vesicles/mL is 2.54×10^{12} , the $E_{\text{curvature}} = 5.24 \times 10^{-6}$ J/mL. Similar calculations for $R = 70$ nm resulted in a curvature energy of $E_{\text{curvature}} = 2.1 \times 10^{-4}$ J/mL. This shows the rather steep dependence of energy on radius. Sonication energy corresponding to the lowest sonication power used, 39 W, was calculated assuming one period of frequency and using the following equation:

$$E = \frac{P \cdot t}{V} \quad (13)$$

where P is the sonication power, t the sonication time and V is the suspension volume (Carolino de Sá and De Lima, 2000). According to Eq. (13) the energy inputted by sonication is $E = 1.95 \times 10^{-4}$ J/mL; therefore, this energy is enough to form liposomes with the radii calculated ($R = 140$ nm). In fact, this value is even close to that obtained for vesicle of 70 nm. Thus, it can be seen the total energy inputted for the ultrasound power is enough to decrease the vesicle size ($E_{\text{curvature}} < E$). However, part of this energy is transformed in calorific energy, as a result, the system temperature increased.

The studied system shows different types of behaviors (Figs. 2 and 3) characterized by one or two relaxation modes. Sonication powers between 39 and 91 W showed a single relaxation mode, which are related with one population of particles. However, two relaxation times were obtained at 130 W of sonication, which could correspond with two different particle size in the system (relation (1) and Eq. (4)). The small particles would be expected considering that the vesicle size decreases when the sonication power increases. The large particles could be hardly associated to liposomes because it would correspond with too big particles. Probably these large particles could be related with metal particles from ultrasound probe due to the strong sonication power, with lipid phase changes or with formation of large lipid aggregates (Zasadzinski, 1986). In relation

with this result, Zasadzinski also reported the formation of different structures when sonication is used to form liposomes. Another fact that makes difficult the analysis of the structures associated to high relaxation times is that large particles mainly contribute at small scattering angles (Callejas-Fernández et al., 2002) and in our experiments the larger relaxation appears only at big scattering angles. The phenomenon of cavitation, induced by sonication, is the basis to the formation of free radicals (Mark et al., 1998). This effect is potentiated at high sonication power. Free radicals could affect the composition of the samples and the formation of different structures that also could be associated to the high relaxation times. These arguments led to fix the power sonication from 39 to 91 W in which DLS curves only show one relaxation mode.

The results shown in Fig. 4, clearly demonstrate a vesicle size decrease as a function of sonication time. The curves could be analogous to the first order kinetic curves following Eq. (14):

$$R = A_0 \exp(-kt) + R_0 \quad (14)$$

the exponential first order fit allows us to obtain the parameters k , R_0 and A_0 (shown in Table 2) where R_0 is the obtained radius, A_0 seems to be related with the initial radius and constant k has similar value in the three cases. In a kinetic reaction the constant k is related with the velocity reaction, in this case by analogy, it could be related with the size decrease velocity which is experimented at the first 1200 s for the three curves. The k values would indicate similar rate of the decrease of the vesicle size for the three powers studied. The kinetic constant is related to the energy barrier. Being the sonication power related with the energy given to the system, a dependence of k with sonication power would be expected. However, our experiments results did not show this behavior.

Smaller final radius could be expected at smaller PC concentrations when fixed times and sonication powers were used. Fig. 5 does not show this effect. A possible explanation could be related with the fact that the concentration of the studied dispersions is not different enough

and the sonication power is distributed analogously in the three systems. All three set of points can be fitted to particle radius dependence,

$$R \propto \frac{1}{\sqrt{P}} \quad (15)$$

This fit is suggested by the form of Eq. (12) if we consider the $E_{\text{curvature}}$ related to the input power P . In any case, precisely because the small different concentration between the samples, we performed only the optimization of sonication time to the 3.75 g/L PC sample. The fact of obtaining similar radii ($R_{3.75} \cong R_{7.5}$) at the concentration range from 3.75 to 7.50 g/L of PC suggests that the sonication time of 3000 s is appropriate.

Hydrolysis of phospholipids is promoted presumably by free radicals in the cavitation bubbles during the preparation of the sonicated phospholipids suspension in water. Thus, during sonication procedure, temperature should be controlled otherwise oxidation and hydrolysis reactions are favored (Almog et al., 1991; Genot et al., 1999). However, it is difficult to guarantee a minimum lipid oxidation level by control of temperature, due to ultrasonic irradiation of water develops hydroxyl free radicals and hydrogen peroxide (Almog et al., 1991). In order to minimize this oxidation we have carried out the process of sonication by sections of 10 min. According to Kruus et al. (1997), the formation of free radicals is not major problems when low frequency (~ 20 kHz) and short sonication times (~ 20 min) are used.

High temperature accelerates PC hydrolysis; however, according to Rabinovich-Guilatt et al. (2005) a temperature of 50 °C during 24 h induce only 1.6% of PC hydrolysis. Therefore, in our working conditions this hydrolysis should be negligible.

Relative standard deviation, obtained by GENDIST, is related with the PI, both of them show a decrease with the increase of sonication power. The highest value of PI, obtained for the lowest sonication power (39 W), is associated with a wide distribution of vesicle radii (Fig. 6). This fact seems indicate that this power (39 W) was not enough to decrease homogeneously the size of particles. However, as we have discussed before, the energy inputted by 39 W of sonication power should be enough to form liposomes with $R = 140$ nm from the initial dispersion $R \approx 300$ nm. Given an initial wide distribution, we can think about a critical radius, R_c , below which the sonication has no effect. Thus, applying a certain sonication power, only the liposomes with radius above R_c would have their size affected by sonication. Clearly, the effect will be not only decrease of the mean radius but also a decrease of polydispersity. Thus, when the vesicle size decreases the energy necessary to keep decreasing

Table 2

Parameters obtained from the first order exponential fit of the curves shown in Fig. 4

Power (W)	A_0 (nm)	R_0 (nm)	k (s ⁻¹)
52	179	106	1/488
78	213	71	1/495
91	227	69	1/482

k is the kinetic constant, R_0 the obtained radius and A_0 is related with the initial radius.

the liposome radius must increase. This could be related with the fact that every sonication power is associated with a minimum radius.

A striking feature can be observed in Fig. 6. The widest curve distribution which corresponds to the minimum sonication power, shows a group of particles smaller in size ($30 \text{ nm} \geq R \leq 60 \text{ nm}$) than those represented in the narrowest curve (maximum sonication power). This fact could be related with the difference between the light scattered by big and small particles (Callejas-Fernández et al., 2002). The high intensity scattered by particles with $R > 60 \text{ nm}$, obtained to 91 W of ultrasound power, indicates a big amount of particles with this size. The contribution of these particles could hinder the particles with $R < 60 \text{ nm}$. In the case of using the minimum sonication power (39 W) the proportion of big particles is lower and for this reason does not hinder particles with $R < 60 \text{ nm}$. Another explanation could be related with the limitation of the GENDIST program. The distribution curve corresponding to the minimum sonication power could be asymmetric and GENDIST program is not able to calculate this type of distribution. We are aware that, in this case, the particles with $30 \text{ nm} \leq R \leq 60 \text{ nm}$ obtained by the low sonication power really represent a smaller amount of particles than those obtained by the high sonication power.

The results obtained by FFEM, shown in Figs. 7 and 8, allow confirming the vesicle size obtained by DLS. In addition, the micrographs allowed obtaining information about the lamellarity of the liposomes system. It is difficult to obtain information related with PI from TEM micrographs because we would need to analyze a big number of images. However, the pictures clearly show the size variability. In agreement with the PI values, this variability is higher in the sample sonicated with 39 W (Fig. 7). The pictures of Fig. 7 show a higher degree of lamellarity than those of Fig. 8. Power sonication of 39 W is not strong enough to decrease homogeneously the lamellarity of vesicles in the sample (Fig. 7). For samples sonicated with 91 W (Fig. 8) we cannot affirm that the liposome dispersion became in a unilamellar system using ultrasound method but we are certain that it is possible to obtain a very low lamellarity system.

This work shows the strong dependence of the system structures with the parameters of sonication. Our results evidence the decrease of the number of lamellae, of the vesicle size and of the PI with the increase of ultrasound power. Thus, the highest sonication power used (91 W) has been functional to obtain a homogenous distribution of lipid vesicles with low lamellarity and low polydispersity at the experimental conditions studied. These findings seem indicate the usefulness of the ultrasound method to

obtain liposomes with low PI. Therefore, this method is an alternative to the extrusion method that has been used before in our group to obtain unilamellar liposomes of PC with similar PI at similar experimental conditions (López et al., 1998a,b).

5. Conclusions

Aqueous lipid dispersions subjected to sonication produce liposomes. The radius of the liposomes is inversely proportional to the square root power, at constant sonication time. This behavior seems to reach a limit at very high power with the detection of multiple decaying signals in the light scattering experiments. The liposome radius decrease as a function of sonication time following an exponential decay behavior. This decay seems independent of the applied power. The plateau radius is reached after about 2200 s of sonication.

The amplitude of the radius distribution function (polydispersity) decreases with the power applied with the same limit obtained for the radius. Electron microscopy observations show a decrease in multilamellarity of the liposomes as a function of power. The results were independent of lipid concentration in the range of concentrations studied (3.75–7.5 g/L of PC). An optimum sonication power and time have been established to produce small liposomes using a sonication probe.

Acknowledgements

The authors wish to thank the expert technical assistance of Dr. Carmen López Iglesias. This work was supported by funds from CICYT (MAT2001-1188-C02-02) and the financial support from the Grant FP-2001-1568.

References

- Almog, R., Forward, R., Samsonoff, C., 1991. Stability of sonicated aqueous suspensions of phospholipids under air. *Chem. Phys. Lipids* 60, 93–99.
- Baszkin, A., Norde, W., 2000. *Physical Chemistry of Biological Interfaces*. Marcel Dekker, NY.
- Callejas-Fernández, J., Tirado-Miranda, M., Quesada-Pérez, M., Odriozola-Prego, G., Schmitt, A., 2002. *Encyclopedia of Surface and Colloid Science*. Marcel Dekker Inc (Chapter Photon Spectroscopy of Colloids, pp. 1–18).
- Carolino de Sá, M.A., De Lima, J.M., 2000. Procedimiento-Padroa para medida da potência liberada pelo aparelho de ultra-som. *Lage G. Ciênc. Agrotec., Lavras* (January/March (4)), 300–306.
- Cladera, J., Rigaud, J.L., Villaverde, J., Duñach, M., 1997. Liposome solubilization and membrane protein reconstitution using Chaps and Chapso. *Eur. J. Biochem.* 243 (3), 798–804.
- Classen, D.E., Spooner, B.S., 1995. Liposome formation in microgravity. *Adv. Space Res.* 17 (6–7), 151–160.

- Cócerca, M., Lopez, O., Estelrich, J., Parra, J.L., de la Maza, A., 2003. Influence of the temperature in the adsorption of sodium dodecyl sulfate on phosphatidylcholine liposomes. *Chem. Phys. Lipids* 124 (1), 15–22.
- Genot, C., Métro, B., Viau, M., Bouchet, B., 1999. Characterisation and stability during storage of liposomes made of muscle phospholipids. *Lebensm.-Wiss. U.-Technol.* 32, 167–174.
- Gregoriadis, G., 1995. Engineering liposomes for drug delivery: progress and problems. *TIBTECH* 13 (12), 527–537.
- Johnson Jr., C.S., Gabriel, A., 1994. *Laser Light Scattering*, first ed. Dover Publications Inc., New York (Chapter 3).
- Jung, H.T., Coldren, B., Zasadzinski, J.A., Iampietro, D.J., Kaler, E.W., 2001. The origins of stability of spontaneous vesicles. *PNAS* 98 (4), 1353–1357.
- Kaasgaard, T., Leidy, C., Crowe, J.H., Mouritsen, O.G., Jorgensen, K., 2003. Temperature-controlled structure and kinetics of ripple phases in one- and two-component supported lipid bilayers. *Biophys. J.* 85 (1), 350–360.
- Kiyoshi, M., Yukio, S., Masao, H., 1992. Formation and mechanical stability of phospholipid vesicles. *Membrane* 17 (4), 257–262.
- Kruus, P., Burk, R.C., Entezari, M.H., Otonari, R., 1997. Sonication of aqueous solutions of chlorobenzene. *Ultrason. Sonochem.* 4, 229–233.
- López, O., de la Maza, A., Coderch, L., López-Iglesias, C., Wehrli, E., Parra, J.L., 1998a. Direct formation of mixed micelles in the solubilization of phospholipid liposomes by Triton X-100. *FEBS Lett.* 426, 314–318.
- López, O., Cócerca, M., Pons, R., Azemar, N., de la Maza, A., 1998b. Kinetic studies of liposome solubilization by sodium dodecyl sulfate based on a dynamic light scattering technique. *Langmuir* 14, 4671–4674.
- Mark, G., Tauber, A., Laupert, R., Schuchmann, H.P., Schulz, D., Mues, A., von Sonntag, C., 1998. OH-radical formation by ultrasound in aqueous solution—Part II: terephthalate and Fricke dosimetry and influence of various conditions on the sonolytic yield. *Ultrason. Sonochem.* 5, 41–52.
- Monnard, P.A., Berclaz, N., Conedes-Frieboes, K., Oberholzer, T., 1999. Decreased solute entrapment in 1-palmitoyl-2-oleoyl-*sn*-glycero-3-phosphocholine liposomes prepared by freeze/thaw in the presence of physiological amounts of monovalent salts. *Langmuir* 15 (22), 7504–7509.
- New, R.R.C., 1990. *Liposomes: A Practical Approach*, first ed. Oxford University Press, pp. 1–33.
- Ollivon, M., Lesieur, S., Grabielle-Madlmont, C., Paternostre, M., 2000. Vesicle reconstitution from lipid-detergent mixed micelle. *Biochim. Biophys. Acta* 1508 (1–2), 34–50.
- Rabinovich-Guilatt, L., Dubernet, C., Gaudin, K., Lambert, G., Couvreur, P., Chaminade, P., 2005. Phospholipid hydrolysis in a pharmaceutical emulsion assessed by physicochemical parameters and a new analytical method. *Eur. J. Pharm. Biopharm.* 61, 69–76.
- Sackmann, E., 1995. In: Lipowsky, R., Sackmann, E. (Eds.), *Handbook of Biological Physics*, vol. 1. Elsevier Science, New York, p. 213.
- Schillén, K., Brown, W., Johnsen, R.M., 1994. Micellar sphere-to-rod transition in an aqueous triblock copolymer system. A dynamic light scattering study of translational and rotational diffusion. *Macromolecules* 27 (17), 4825–4832.
- Teschke, O., de Souza, E.F., 2002. Liposome structure imaging by atomic force microscopy: verification of improved liposome stability during adsorption of multiple aggregated vesicles. *Langmuir* 18 (17), 6513–6520.
- Traïkia, M., Warschawski, D.E., Recouvreur, M., Cartaud, J., Devaux, P.F., 2000. Formation of unilamellar vesicles by repetitive freeze-thaw cycles: characterization by electron microscopy and P-31-nuclear magnetic resonance. *Eur. Biophys. J. Biophys.* 29 (3), 184–195.
- Zasadzinski, A.N., 1986. Transmission electron microscopy observations of sonication-induced changes in liposome structure. *Biophys. J.* 49, 1119–1130.